Physical effects of biologically formed cholesterol oxidation products on lipid membranes investigated with fluorescence depolarization spectroscopy and electron spin resonance

J. C. D. Verhagen,* P. ter Braake,* J. Teunissen,* G. van Ginkel,[1,*] and A. Sevanian[†]

Department of Molecular Biophysics,* Debye Research Institute, Utrecht University, Buys Ballot Laboratory, Princetonplein 5, Utrecht 3584 CC, The Netherlands, and Department of Molecular Pharmacology and Toxicology,[†] School of Pharmacy, University of Southern California, 1985 Zonal Avenue, Los Angeles, CA 90033-1086

Abstract Planar oriented membranes of 1-palmitoyl, 2-oleoyl-phosphatidylcholine (POPC) containing cholesterol, 19-hydroxycholesterol, 22S-hydroxycholesterol, or 25-hydroxycholesterol in concentrations up to 5 mol % were investigated with angle-resolved fluorescence depolarization and electron spin resonance measurements. Analyses of the data with the Brownian diffusion model show that the oxysterols have structural effects similar to those of cholesterol: an increase in molecular order and no change in the rotational diffusion coefficients of the probe molecules. Time-resolved fluorescence anisotropy measurements on diphenylhexatriene (DPH) in small unilamellar vesicles of POPC and DOPC were performed using oxysterols commonly found in oxidized low density lipoproteins (LDL) in comparison to membranes containing cholesterol or no sterols. Analyses using the Brownian rotational diffusion model show that most LDL-oxysterols affect the vesicle physical structure in a manner similar to cholesterol, viz. an increase in molecular order and a decrease in the dynamics. Cholesterol-α-epoxide has a much smaller ordering effect than cholesterol in POPC-vesicles. A similar effect was found for 7β-hydroxycholesterol in DOPC-vesicles. The tendency of the oxysterols to influence the molecular order as compared to pure cholesterol may contribute to cell membrane permeability changes affecting crucial cell functions and events leading to vascular cell injury. Increased LDL oxysterol levels may account for some of the structural changes noted for oxidatively modified LDL as well as its toxicity to vascular cells.—**Verhagen, J. C. D., P. ter Braake, J. Teunissen, G. van Ginkel, and A. Sevanian.** Physical effects of biologically formed cholesterol oxidation products on lipid membranes investigated with fluorescence depolarization spectroscopy and electron spin resonance. *J. Lipid Res.* 1996. **37:** 1488–1502.

Supplementary key words cholesterol oxides • oxysterols • hydroxycholesterol • cholestanetriol • ketocholesterol • membrane oxidation • LDL oxidation • atherogenesis

Cholesterol is a common constituent of mammalian cell membrane lipids. In some membranes cholesterol is the single most prevalent lipid (1, 2) and plays an important, although not fully understood, role in maintaining membrane structural integrity and function. There are many studies which show that cholesterol has a condensing and strong ordering effect on membranes and that its presence in membranes restricts permeability to a range of compounds. Moreover, it has been reported that the condensing effect of cholesterol also affects the activity of certain membrane bound proteins (for a review see ref. 3).

Cholesterol is known to become readily oxidized under certain conditions, particularly in regard to peroxidation reactions initiated by metabolically derived reactive oxygen species (1, 2, 4). During such oxidative reactions a variety of cholesterol oxidation products (oxysterols) are formed (1, 2, 4), some of which have been shown to be highly cytotoxic (5–8). Although the exact nature of their toxicity requires further study,

Abbreviations: ADC, analogue-to-digital converter; AFD, steady-state angle-resolved fluorescence depolarization; CO-mix, mixture of oxysterols found in oxidized LDL (see Table 1); CSL, 3-doxyl-5α-cholestane; CW-ESR, continuous wave electron spin resonance; DOPC, 1,2-dioleoyl-phosphatidylcholine; DPH, 1,6-diphenyl-1,3,5-hexatriene; ESR, electron spin resonance; LDL, low density lipoprotein; POPC, 1-palmitoyl-2-oleoyl-phosphatidylcholine; SLE, stochastic Liouville equation; TMA-DPH, 1-(trimethyl-ammonium)-1,6-diphenyl-1,3,5-hexatriene.

[1]To whom correspondence should be addressed.

Downloaded from www.jlr.org by guest, on June 18, 2012

some of the cytotoxicity observed in cell culture studies appears to be due to effects on membranes (9) where pronounced effects on the physical properties of lipid membranes have been noted (10). Other related effects include interactions with specific proteins, thereby changing their functional properties (9–11). Oxysterols also have a strong effect on the rate of aggregation of blood platelets (12). The molecular mechanism of this process is not well understood.

Recently, increasing evidence has become available which indicates that oxysterols are found in plasma lipoproteins in considerable amounts (11) and may be generated by oxidative reactions acting on low density lipoproteins (LDL) in the vessel wall (13, 14) or the circulation (13, 15, 16). The presence of these oxysterols may serve as a marker of oxidative modification and also as a contributing factor in the atherogenicity ascribed to oxidatively modified LDL. Several oxysterols are found in LDL and are markedly elevated in hypercholesterolemic subjects (17, 18). Oxysterols are also found in arteries with human arteriosclerotic plaque, while they are absent in normal arteries (19).

Although the cytotoxic effects of oxysterols are different for the different oxysterols and in some cases this cytotoxicity is expressed after some time of exposure (4, 6, 9) it seems reasonable to assume that the early effects of oxysterols on cell function are associated with their action on membranes. In the present study we investigated the physical effects of specific oxysterols on model lipid membranes, concentrating on some oxysterols that have strong effects on the aggregation of blood platelets and on the oxysterols found in oxidized LDL. To this end we used the well-known techniques of fluorescence depolarization spectroscopy and electron spin resonance. The advantage of these techniques lies in their sensitivity to molecular motions on the time-scale of the dynamics of lipid molecules in membranes (1–100 ns) and that structural information is obtained on a microscopic scale, i.e., molecular orientational distribution of the probe molecules from the determined order parameters of the probes (20–25).

For the study of the structural effects of oxysterols that affect the rate of blood platelet aggregation, we used steady-state angle-resolved fluorescence depolarization spectroscopy and CW-ESR on planar oriented membranes of POPC containing known quantities of different oxysterols. For comparison, planar bilayers of pure POPC and POPC with cholesterol were studied. TMA-DPH and CSL were used as probe molecules and have been shown to yield very similar results in planar lipid bilayers; both molecules are rod-shaped and have a polar head group that keeps them anchored at the lipid–water interface (21). Time-resolved fluorescence anisotropy measurements on small unilamellar vesicles of POPC and DOPC were performed to study the structural effects of oxysterols found in oxidized LDL. For these investigations we used the apolar probe DPH.

The three techniques used in this study, AFD, CW-ESR and time-resolved fluorescence depolarization spectroscopy, yield essentially the same structural physical parameters, namely the order parameters and the rotational diffusion coefficients of the probe molecules in the investigated membranes. The interpretation of the dynamics of the probe molecules in the membranes is dependent on the physical reorientational model that is imposed on the experimentally established ESR spectra, the AFD data and fluorescence anisotropy decay curves. Different models have been proposed in the literature and a model that is frequently used is the so called Brownian diffusion model (26, 27). This model is feasible from a physical point of view and it generally gives a good fit to the experimental data derived from model lipid membranes.

Although the three investigation techniques we used yield essentially the same parameters, the absolute values of the determined parameters may differ because of the differences in probe characteristics and because of the differences in membrane curvature and water content between the planar oriented lipid samples on the one hand and the small unilamellar lipid vesicles on the other hand.

MATERIALS AND METHODS

Chemicals

The phospholipids, 1-palmitoyl-2-oleoyl-phosphatidylcholine (POPC) and 1,2-dioleoyl-phosphatidylcholine (DOPC) were purchased from Avanti Polar Lipids (Alabaster, AL) and used without further purification. DPH and TMA-DPH were purchased from Molecular Probes (Eugene, OR). The ESR probe, 3-doxyl-5α-cholestane (CSL) was bought from Aldrich Chemical Company. Stock solutions at concentrations of $5 \cdot 10^{-4}$ M in pure ethanol were stored under nitrogen in the dark at 4°C. All oxysterols described in this report, as well as cholesterol, were purchased from Steraloids, Inc. (Wilton, NH). The oxysterols studied include: cholest-5-ene-3β,7α-diol (7α-hydroxycholesterol), cholest-5-ene-3β,7β-diol (7β-hydroxycholesterol), 5,6α-epoxy-5α-cholestan-3β-ol (cholesterol-α-epoxide),5-α-cholestane-3β,5,6β-triol (cholestanetriol), 3β-hydroxycholest-5-ene-7-one (7-ketocholesterol), 5,6β-epoxy-5β-cholestan-3β-ol (cholesterol-β-epoxide), cholesta-3,5,diene-7-one (3,5-diene-7-one), cholest-5-ene-3β,25-diol (25-hydroxycholesterol), cholest-5-ene-3β,19-diol (19-hydroxycholesterol), cholest-5-ene-3β,22-diol (22S-hydroxycholesterol). Trivial names are

Downloaded from www.jlr.org by guest, on June 18, 2012

indicated in parentheses. We have listed the structures of the different oxysterols in comparison to cholesterol in **Figure 1.**

Preparation of lipid vesicles

Lipid vesicles were made by mixing 4 mg of phospholipid with appropriate amounts of the probe solution to yield a final lipid to probe ratio of 250:1 on a molar basis for fluorescence depolarization experiments. The lipid–probe mixture was dried under a stream of oxygen-free nitrogen and remaining traces of solvent were removed by application of high vacuum for 6–8 h at room temperature. Vesicles containing specified amounts of oxysterols were prepared in the same manner. The dried lipids were then dispersed in 6 ml Tris-EDTA (20 mM Tris, 0.75 mM EDTA) buffer, pH 7.8, sparged with nitrogen gas. After vortexing the lipid suspension for 30 sec, the samples were subjected to sonication using a bath-type sonicator for 30–45 min in the dark under a nitrogen atmosphere. Attempts to prepare POPC vesicles containing oxysterols using extrusion techniques (28) were unsuccessful due to absorption of the oxysterols to the filters of the extrusion equipment. Gas chromatographic analyses of the extruded POPC-oxysterol (29) vesicles showed that only about 20% of the added oxysterols was incorporated upon extrusion. We therefore concluded that the extrusion technique is not suitable for preparing well-defined POPC-oxysterol vesicles.

Suspensions that were not optically clear upon sonication were centrifuged for 1 h at 50,000 *g* in a high-speed refrigerated centrifuge and the resulting super-

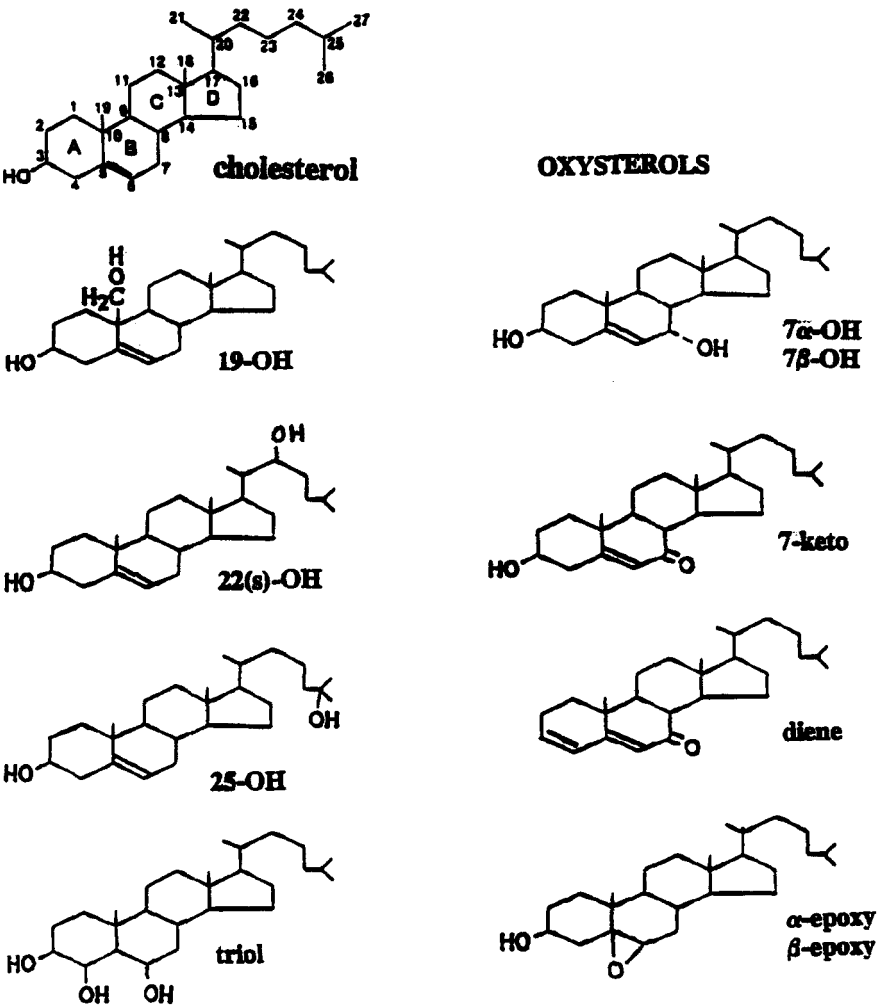

Fig. 1. Structural formulas of cholesterol and the oxysterols used in this study: 19-OH, 19-hydroxycholesterol; 22(s)-OH, 22S-hydroxycholesterol; 25-OH, 25-hydroxycholesterol; triol, cholestanetriol; 7α-OH, 7α-hydroxycholesterol; 7β-OH, 7β-hydroxycholesterol; 7-keto, 7-ketocholesterol; diene, 3,5-diene-7-one; α-epoxy, cholesterol-α-epoxide; β-epoxy, cholesterol-β-epoxide.

Downloaded from www.jlr.org by guest, on June 18, 2012

natant was used for further studies. In some experiments a mixture of the oxysterols was prepared and incorporated in the lipid vesicles. This mixture approximates the relative proportion of the oxysterols found in LDL as reported by Hodis et al. (11) and is listed in **Table 1.** The oxysterol content of the vesicles was checked by extraction of aliquots and analysis by gas chromatography (29).

Preparation of stacked planar bilayers

Planar oriented multibilayers were made by mixing 8 mg of phospholipid with appropriate amounts of the probe solution to yield a final probe to lipid to probe ratio of 250:1 on a molar basis for the AFD samples and 100:1 for the ESR samples. The lipid–probe mixture was dried under a stream of nitrogen. The resulting dry mixture was allowed to equilibrate with water vapor above a saturated solution of K_2SO_4 (96% relative humidity) overnight under a strict nitrogen atmosphere. Planar oriented multibilayers were prepared by gently rubbing the hydrated lipid mixture between two microscope glass coverslips. The alignment was checked by a polarizing microscope with a first-order red plate. After alignment, the samples were hydrated above the solution of K_2SO_4 overnight to compensate for water losses during the alignment. After this hydration the edges of the samples for AFD measurements were sealed with two-component epoxy resin to prevent dehydration. The contribution of scattered excitation was minimized by completely blacking the samples except for a circular area 4 mm in diameter (22). The ESR samples were kept in a nitrogen atmosphere in a quartz tube containing a solution of saturated potassium sulfate.

Steady-state angle-resolved fluorescence depolarization experiments

Angle-resolved fluorescence depolarization experiments were performed with a home-built fluorimeter. The excitation light was set at 362 ± 5 nm with a Bausch and Lomb monochromator and an interference filter.

TABLE 1. Relative proportions of oxysterols in oxidized LDL

Compound	%
7α-Hydroxycholesterol	5.4
7β-Hydroxycholesterol	20.2
Cholesterol-β-epoxide	16.8
Cholesterol-α-epoxide	24.2
Cholestanetriol	5.4
7-Ketocholesterol	24.8
25-Hydroxycholesterol	3.2

Relative proportions of oxysterols in oxidized LDL, from Hodis et al. (11).

The emission wavelength was selected with a 438 ± 7 nm interference filter (Balzer) together with an LF-40 low cut-off filter (Schott). The signal was detected with a Phillips XP2020Q photomultiplier. The signal from the multiplier was fed to a Lock-in amplifier (Princeton Applied Research 124A) and converted into digital form using a 12-bit ADC. In the extraordinary experiment performed here the polarization intensity ratio is determined for 56 different combinations of excitation and emission angles.

Continuous wave electron spin resonance experiments

Electron spin resonance experiments (ESR) were performed with a Varian E-9 X-band spectrometer, equipped with a TM110 cavity. The sample was placed in a quartz tube above a saturated salt solution to maintain the water concentration and in a nitrogen atmosphere to prevent oxidation. The orientation of the sample director relative to the applied static magnetic field was varied using a home built goniometer. ESR spectra were recorded at a microwave power level of 1 to 2 mW, well below saturation. A magnetic field modulation of 1 Gauss (top-top) with a frequency of 100 kHz was used to detect the derivative of the absorption signal. The background ESR signal, arising from the quartz tube and the glass plates, was subtracted from the measurements before analysis.

Time-resolved fluorescence depolarization measurements

Time-resolved fluorescence depolarization experiments were performed with the Synchrotron Radiation Source (SRS) in Daresbury (U.K.) operating in single bunch mode at a 3 MHz repetition rate with a 250 ps pulse width. The excitation wavelength was set at 358 ± 3 nm with a SPEX monochromator. A 438 ± 7 nm interference filter (Balzers) together with an LF-40 cut-off filter (Schott) were used for fluorescence emission wavelength definition. The standard electronic setup was used for time-correlated single photon counting as described previously (20). Unless stated otherwise, all experiments were done at ambient room temperature (20 ± 2°C). Complete decay curves of the fluorescence intensity in parallel and perpendicular polarization were recorded within the range of 1022 channels of the multichannel analyzer; channel widths of 20 ps/channel were used. The excitation flash profile was obtained from the elastic scattering of the vesicle sample monitored at the emission wavelength of 438 nm.

Description of the spectroscopic methods

Information on both structural organization and molecular dynamics within a lipid bilayer is accessible by fluorescence depolarization as well as electron spin reso-

Downloaded from www.jlr.org by guest, on June 18, 2012

TABLE 2. Effects of oxysterols on molecular order and dynamics of CSL in planar POPC bilayers: ESR measurements

Lipid	$\langle P_2 \rangle$	$\langle P_4 \rangle$	$D_{\|}$ (1/ns)	$D_{\perp}$ (1/ns)	T (°C)
POPC	0.63	0.27	1.2	1.2	21
POPC	0.59	0.23	2.0	2.0	35
POPC	0.54	0.19	3.5	3.5	45
POPC + cholesterol	0.73	0.39	0.8	0.8	21
POPC + cholesterol	0.65	0.29	2.5	3.0	35
POPC + cholesterol	0.57	0.22	3.0	4.0	45
POPC + 19-hydroxycholesterol	0.69	0.34	1.2	1.2	21
POPC + 19-hydroxycholesterol	0.66	0.30	2.0	1.8	35
POPC + 19-hydroxycholesterol	0.60	0.24	3.0	2.0	45
POPC + 22S-hydroxycholesterol	0.70	0.35	1.3	1.3	21
POPC + 22S-hydroxycholesterol	0.64	0.28	2.0	2.0	35
POPC + 22S-hydroxycholesterol	0.63	0.27	2.9	2.9	45
POPC + 25-hydroxycholesterol	0.70	0.38	1.0	1.0	21
POPC + 25-hydroxycholesterol	0.66	0.34	1.8	2.2	35
POPC + 25-hydroxycholesterol	0.63	0.32	3.0	3.0	45

Structural affects of cholesterol and the indicated oxysterols on planar POPC bilayers investigated by angle-resolved continuous wave ESR. A POPC:cholestane spin label (CSL) ratio of 100:1 was used. Cholesterol and oxysterols are present at a concentration of 5 mol %. The effects are listed by the order parameters $\langle P_2 \rangle$ and $\langle P_4 \rangle$ as well as by the dynamic parameters $D_{\|}$and $D_{\perp}$. Visually judged quality of fit: 15% in $\langle P_2 \rangle$, 25% in $\langle P_4 \rangle$, and 30% in $D_{\perp}$.

nance spectroscopy. Both techniques provide only indirect information in that they study the response of fluorescent or paramagnetic probe molecules that have been added in low concentration to the lipid system under study. In time-resolved fluorescence depolarization experiments the sample is irradiated with flashes of monochromatic incoherent polarized light, and in AFD experiments the sample is irradiated with steady-state monochromatic incoherent polarized light. In both methods the incoming light preferentially excites those fluorescent probe molecules whose absorption moment is aligned more parallel to the electric field component of the incoming light. The excited molecules relax to their ground state with a characteristic fluorescence decay time τ_F by emitting a photon polarized in the plane containing the emission moment. Structural information on the average orientations of the probe in the lipid bilayer is obtained by studying the selectivity of the absorption and the fluorescence depolarization process. Dynamic information is obtained by measuring the extent of depolarization of the emitted radiation. The latter is caused by reorientation of the emission moment due to molecular motions in the short time interval between the absorption and emission processes. Obviously, this method is sensitive for dynamic processes that induce loss of orientation correlation and for which the characteristic correlation time is of the order of the fluorescence decay time τ_F. The fluorescence decay time of DPH and TMA-DPH in lipid bilayers is in the range of 3–10 ns. The theoretical description of time-resolved fluorescence depolarization and AFD experiments has been elaborated (20, 22–25). The process of molecular tumbling is described by the so-called Brownian rotational diffusion model. This model incorporates two types of anisotropy that characterize the tumbling motion of the fluorescent probe. The first is motional anisotropy, as expected for a particle with nonspherical shape, where the rotational diffusion around the long molecular axis should be faster than the tumbling of the axis itself. This implies a description with two diffusion rates $D_{\|} > D_{\perp}$ for motions around and of the long molecular axis respectively. D is defined as the variance of the rotation angle divided by the rotation time. Second, it incorporates the anisotropy due to the surrounding lipid matrix, which is a reflection of the microscopic order inside the lipid bilayer. This implies a microscopic orientation distribution function P_{eq} for the fluorescent probes, which is conveniently parametrized by an ordering potential U:

$$P_{eq}(\Omega) = e^{-U(\Omega)}/\int e^{-U(\Omega)}\, d\Omega \qquad \textit{Eq. 1)}$$

and is normalized to unity under integration over all molecular orientations with respect to the bilayer normal. This distribution is the unique stationary mode of the Brownian diffusion process. For the average potential U we use

$$U(\Omega) = U(\alpha,\beta,\gamma) = \lambda_2 P_2(\cos\beta) + \lambda_4 P_4(\cos\beta) \qquad \textit{Eq. 2)}$$

which depends only on the Euler angle β between the bilayer normal and the long axis of the molecule. In the Brownian diffusion framework, therefore, the molecular tumbling process is characterized by four parameters λ_2, λ_4, $D_{\|}$, $D\perp$. Dependence on the last of these is

Downloaded from www.jlr.org by guest, on June 18, 2012

negligible for situations where the absorption moment is nearly parallel with the long axis of the fluorescent probe as is the case with DPH and TMA-DPH. The analysis of the experimental data proceeds with a fitting algorithm for the three remaining parameters based on the numerical solution of the Brownian diffusion problem in terms of angular eigenfunctions and their characteristic correlation times. Details of this numerical procedure are given in ref. 30. Information on the average microscopic probe distribution is obtained in the form of optimal values for λ_2 and λ_4. It is customary, however, to characterize molecular order not in terms of these parameters or the distribution function itself but rather in the first even weighted averages of the Legendre polynomials:

$$P_2 = 1/2(\cos^2 \beta - 1) \qquad \textit{Eq. 3)}$$

$$P_4 = 1/8(35\cos^4 \beta - 30\cos^2 \beta + 3) \qquad \textit{Eq. 4)}$$

$$\langle P_n \rangle = \int P_{eq}(\Omega) P_n(\cos \beta) d\Omega \quad (n=2,4...) \qquad \textit{Eq. 5)}$$

In ESR spectroscopy, one observes radiative transitions between energy levels, the splitting of which is not determined by internal molecular structure, as with fluorescence depolarization, but rather by application of a static external magnetic field. The probes used are paramagnetic amphiphiles, i.e., stable radicals that embed themselves in the membrane. Under magnetic field, the unpaired electron of the probe exhibits a Zeeman splitting typically corresponding to microwave radiation in the 10-GHz-range (X-band). In contrast to the fluorescence process, the relaxation is non-radiative and leads to detectable absorption of the microwave radiation. For the relevant cases, this Zeeman coupling is anisotropic, i.e., the absorption frequency depends on the molecular orientation with respect to the magnetic field. A variety of orientations of the probes thus leads to non-homogeneous broadening of the absorption line shape. Clearly, structural information on preferred orientations of the ESR probe may be obtained by inspecting the relative weights of the various frequencies in the total line shape, i.e., detailed line-shape analysis. Dynamic information may be obtained also. This follows from the observation that, under extremely fast reorientational motion, the Zeeman interaction may be replaced by its orientational average. The latter leads to a single averaged absorption frequency, implying a single, narrow absorption line. Closer inspection reveals that this line-width collapse will occur for reorientation correlation times τ near the inverse line width $\Delta\omega$: $\Delta\omega\tau \approx 1$. For the most common nitroxide spin probes as used in this work, the typical line width is about 5 ns.

In contrast to the previous case of fluorescence depolarization, the theoretical description not only incorporated the stochastic tumbling motion but deterministic time development of the Zeeman Hamiltonian as well. A suitable mathematical framework has been developed in the form of the so-called stochastic Liouville equation (SLE) (21, 30–33). Its numerical solution proceeds via eigenfunction expansions. The experimental ESR spectra are then analyzed by solving the SLE with the application of the Brownian diffusion model mentioned above. Just as in the case of fluorescence depolarization, the tumbling operator is parametrized in terms of rotational diffusion rates $D_\parallel$ and $D_\perp$ for motions around the long molecular axis and of the long molecular axis, respectively. Aside from this motional anisotropy, the SLE also accounts for anisotropy of the surrounding lipid matrix. The expression for the orientational distribution function in the bilayer is identical for the ESR experiments and for the fluorescence depolarization experiments (see equations 1 and 2). The magnetic coupling of the nitroxide probes were taken to be a standard Zeeman coupling with hyperfine splitting due to the nitrogen nuclear spin. The diagonal elements of the coupling tensors were taken as g = diag (2.0081, 2.0024, 2.0061) and A = diag (5.3, 33.8, 5.1). The fits of the ESR lineshapes were performed as described (21, 31), with quality of the fit being judged visually.

For the three techniques described, the order parameters $\langle P_2 \rangle$ and $\langle P_4 \rangle$ were determined from the established λ_2 and λ_4 values. The uncertainties in $\langle P_2 \rangle$, $\langle P_4 \rangle$, and the diffusion coefficient $D_\perp$ for the AFD and time-resolved anisotropy were determined from the 68% confidence level in the $\langle P_2 \rangle$, $\langle P_4 \rangle$, $D_\perp$-hyperplane and were found to be 15%, 25%, and 30%, respectively (34), a method similar to the one used by Beechem (35). We estimate from the visual judgement of the fits (21, 31) of the ESR-spectra that the extracted values of $\langle P_2 \rangle$, $\langle P_4 \rangle$, $D_\perp$ and $D_\parallel$ are reliable within the following bounds: $\langle P_2 \rangle$: 10%, $\langle P4 \rangle$: 20%, $D\perp$: 25%, and $D_\parallel$: 30%.

As mentioned earlier, the three spectroscopic techniques used in this study, AFD and CW-ESR on planar oriented membranes and time-resolved fluorescence depolarization spectroscopy on small unilamellar lipid vesicles, yield essentially the same parameters, namely, the order parameters $\langle P_2 \rangle$ and $\langle P_4 \rangle$ and the rotational diffusion coefficients of the probe molecules. However, the absolute values of these parameters may differ because of the differences in probe characteristics and because of the differences in membrane curvature and water content between the planar oriented membranes on the one hand and the small unilamellar lipid vesicles on the other hand.

RESULTS

As indicated earlier, it seems reasonable to assume that early effects of oxysterols on cell function could be due partly to the structural effects of these compounds

Downloaded from www.jlr.org by guest, on June 18, 2012

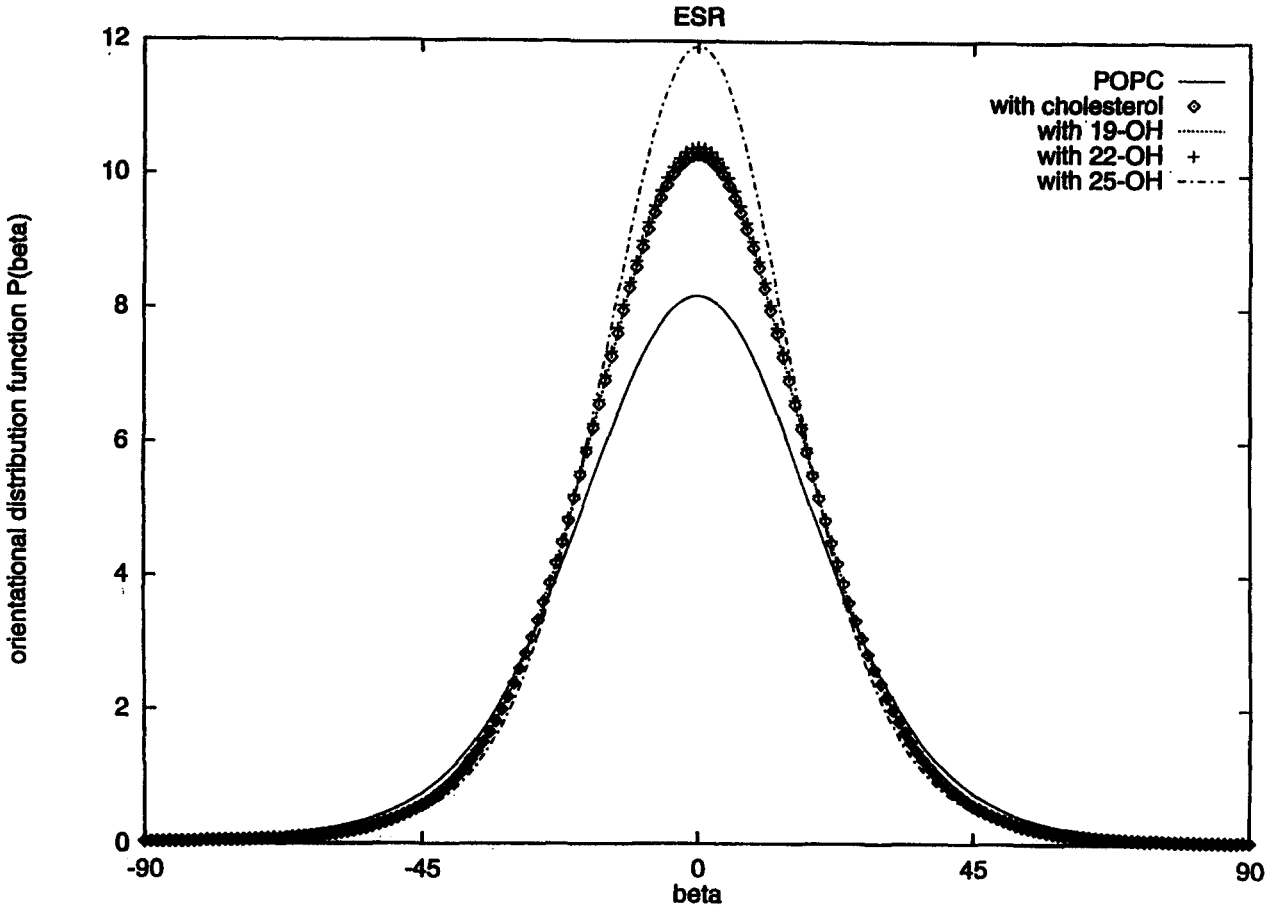

Fig. 2. Orientational distribution functions P(β) of CSL in stacked planar bilayers of POPC, POPC + cholesterol, POPC + 19-hydroxycholesterol, POPC + 22S-hydroxycholesterol, and POPC + 25-hydroxycholesterol measured at 35°C. A sterol to phospholipid ratio of 1:20 was used. The effects of oxysterols in the planar bilayers were investigated using ESR measurements on the spin probe CSL using a lipid to probe ratio of 100:1 (see also Table 2).

on the membranes containing the oxysterols. We, therefore, decided to investigate well-defined model membranes consisting of POPC and DOPC, lipid species that are commonly found in human and animal cell membranes. Their biophysical characteristics are well described in connection with the characterization of the probe molecules used (20–25).

In a study by Blache and Bontoux (12) it was shown that 22S-hydroxycholesterol in rat platelets strongly enhances the rate of platelet aggregation, whereas 25-hydroxycholesterol strongly decreases it. These puzzling results stimulated us to study the physical effects of these oxysterols in model lipid membranes. We also studied the effect of 19-hydroxycholesterol to explore whether the position of the hydroxy group on the sterol skeleton of the oxysterol in the membrane affects the structural properties of the membrane. For these investigations we performed ESR measurements on CSL and AFD measurements on TMA-DPH in planar-oriented POPC membranes containing known quantities of the oxysterols 22S-hydroxycholesterol, 25-hydroxycholesterol, and 19-hydroxycholesterol. For comparison, planar bilayers of pure POPC and POPC + cholesterol were also investigated.

ESR measurements on planar POPC bilayers

The results of the CW-ESR measurements on planar POPC membranes are listed in **Table 2.** In this table are listed the effects of 5 mol % of cholesterol, 19-hydroxycholesterol, 22S-hydroxycholesterol, and 25-hydroxycholesterol on the order parameters and the rotational diffusion coefficients of the spinprobe CSL at 21°, 35°, and 45°C. These data were obtained upon application of the Brownian rotational diffusion model for simulation of the measured ESR spectra. Table 2 shows that 19-hydroxycholesterol, 22S-hydroxycholesterol, and 25-hydroxycholesterol have the same structural effects on planar POPC membranes as cholesterol, namely, an increase in molecular order and no change in the dynamical parameters. The similarity of the ordering ef-

Downloaded from www.jlr.org by guest, on June 18, 2012

TABLE 3. Effects of oxysterols on molecular order and dynamics of TMA-DPH in planar POPC bilayers: AFD measurements

Lipid	Sterol Conc. (mol %)	$\langle P_2 \rangle$	$\langle P_4 \rangle$	$D_\perp \langle \tau \rangle$
POPC	0	0.60	0.29	0.12
POPC + cholesterol	2.5	0.63	0.32	0.13
POPC + cholesterol	5	0.65	0.34	0.14
POPC + cholesterol	10	0.70	0.40	0.12
POPC + cholesterol	20	0.74	0.45	0.11
POPC + 19-hydroxycholesterol	2.5	0.61	0.29	0.12
POPC + 19-hydroxycholesterol	5	0.64	0.33	0.11
POPC + 19-hydroxycholesterol	10	0.66	0.39	0.12
POPC + 22S-hydroxycholesterol	2.5	0.63	0.33	0.12
POPC + 22S-hydroxycholesterol	5	0.70	0.39	0.09
POPC + 25-hydroxycholesterol	2.5	0.63	0.33	0.12
POPC + 25-hydroxycholesterol	5	0.68	0.40	0.16

Structural effects of cholesterol and the indicated cholesterol oxides on planar POPC bilayers investigated with angle-resolved fluorescence depolarization measurements using TMA-DPH. The ratio POPC:TMA-DPH was 250:1. All experiments were performed at 21° ± 2°C. The structural effects are listed in the form of the order parameters $\langle P_2 \rangle$ and $\langle P_4 \rangle$ and by the dynamic parameter $D_\perp \langle \tau \rangle$, where $D_\perp$ stands for the wobbling diffusion coefficient of the long molecular axis and $\langle \tau \rangle$ is the average fluorescence lifetime of TMA-DPH. The uncertainties (68% confidence limits) are 15% in $\langle P_2 \rangle$, 25% in $\langle P_4 \rangle$, and 30% in $D_\perp$.

fects of the three investigated oxysterols with cholesterol are also shown in **Fig. 2** where we have plotted the orientational distribution function of CSL at 35°C in the POPC membranes with cholesterol and the different oxysterols.

AFD measurements on planar POPC bilayers

The structural effects of the oxysterols 19-hydroxycholesterol, 22S-hydroxycholesterol, and 25-hydroxycholesterol were also investigated by AFD on planar POPC membranes at 21°C in comparison with planar membranes of pure POPC and POPC + cholesterol. TMA-DPH was used as the probe molecule. The results of the analysis with the Brownian rotation diffusion model are listed in **Table 3.** As shown in Table 3, we have studied the structural effects of different concentrations of oxysterols in comparison with cholesterol. Concentrations of 2.5, 5, 10, and 20 mol % of cholesterol and oxysterols were investigated. For some oxysterols, however, it was not possible to incorporate concentrations higher than 5 mol %, because at these higher concentrations we could not get uniformly aligned lipid bilayers. Table 3 shows that 19-hydroxycholesterol, 22S-hydroxycholesterol, and 25-hydroxycholesterol have the same structural effects on planar POPC bilayers as cholesterol, namely, an increase in molecular order and no change in the dynamics of TMA-DPH, in agreement with the ESR results shown in Table 2. The ordering effects are also illustrated by **Fig. 3** where we have plotted the orientational distribution functions of TMA-DPH in the planar POPC bilayers with cholesterol and the oxysterols. The dynamic parameters in Table 3 are listed as the product of the rotational diffusion coefficient $D_\perp$ and the average fluorescence lifetime of TMA-DPH, that is, the resulting parameter from the analysis of the steady-state AFD data. The value of $D_\perp$ can be calculated when the fluorescence decay curve of TMA-DPH in the planar POPC bilayers is known. In previous studies we have determined how the average fluorescence lifetime $\langle \tau \rangle$ of TMA-DPH is affected by high cholesterol concentrations (25 mol %). In planar POPC bilayers $\langle \tau \rangle$ changes from 4.55 to 5.38 ns due to the presence of cholesterol (24) while in POPC vesicles it changes from 4.00 to 5.99 ns under the influence of 25 mol % cholesterol (36). We have determined the average fluorescence lifetime of TMA-DPH in POPC vesicles and in POPC vesicles containing 5 mol % cholesterol or 25-hydroxycholesterol, see **Table 4.** This table shows that within experimental error these sterol concentrations do not affect the average fluorescence lifetime of TMA-DPH. From this observation we conclude that the diffusion coefficient of TMA-DPH is not affected by 5 mol % of cholesterol or 25-hydroxycholesterol. Although we have not determined the fluorescence lifetime of TMA-DPH in POPC bilayers containing 19-hydroxycholesterol or 22S-hydroxycholesterol, we think that it is justified to assume that the latter oxysterols also will not change the lifetime of TMA-DPH in these low concentrations. This assumption is supported by the observation that the average fluorescence lifetime of DPH in POPC and DOPC is not affected by addition of 5 mol % cholesterol or oxysterols from oxidized LDL (see next section and Table 5).

If the oxysterols do not affect the fluorescence decay curve of TMA-DPH significantly as compared with cholesterol, which seems a reasonable assumption as outlined above, then it is safe to conclude that the dynamics of TMA-DPH in the presence of the oxysterols does not

Downloaded from www.jlr.org by guest, on June 18, 2012

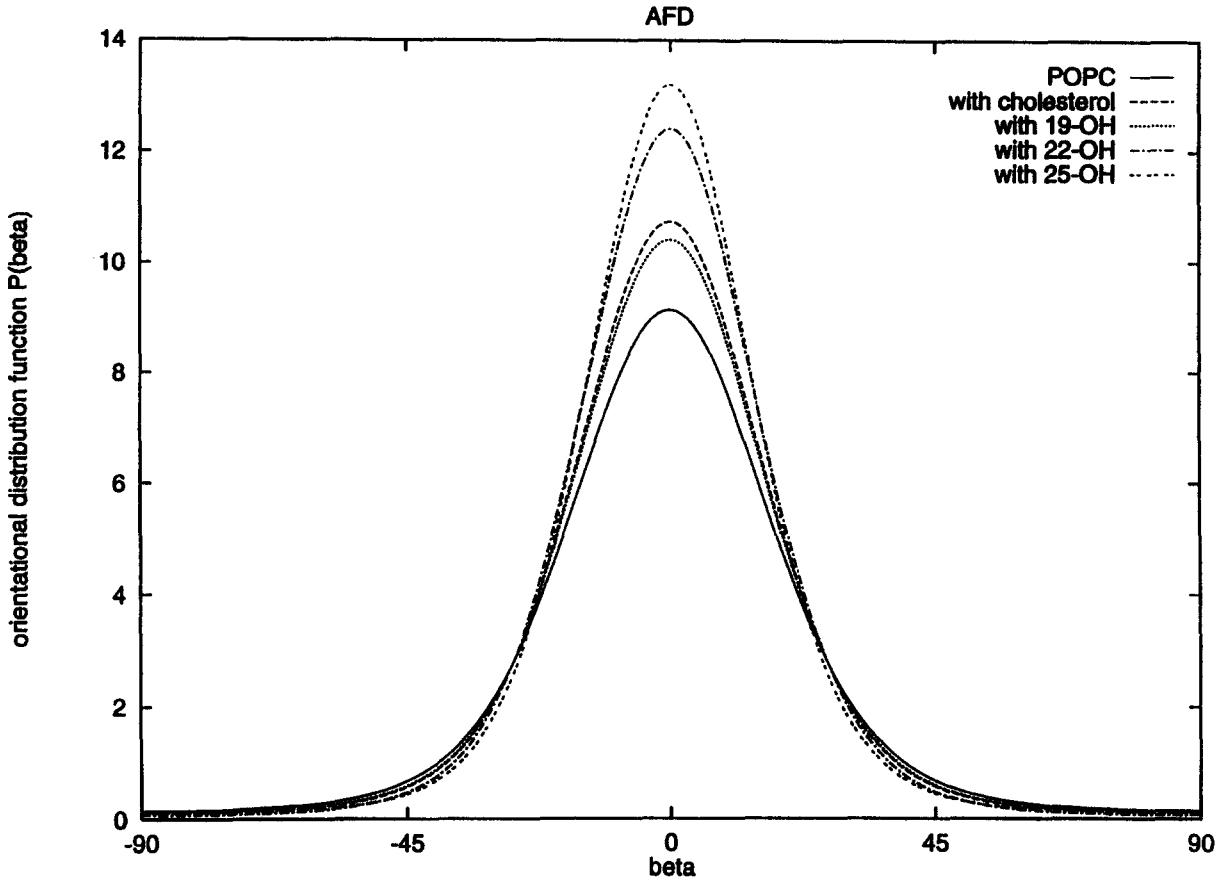

Fig. 3. Orientational distribution functions P(β) of TMA-DPH in stacked planar bilayers of POPC, POPC + cholesterol, POPC + 19-hydroxycholesterol, POPC + 22S-hydroxycholesterol, and POPC + 25-hydroxycholesterol measured at 20°C. A sterol to phospholipid ratio of 1:20 was used. The effects of oxysterols in the planar bilayers were investigated using AFD measurements on the fluorescent probe TMA-DPH using a lipid to probe ratio of 250:1 (see also Table 3).

change in comparison with the probe dynamics brought about by cholesterol. This is in line with the ESR data from Table 2.

Time-resolved fluorescence depolarization measurements on small unilamellar POPC lipid vesicles

The membrane structural effects of oxysterols commonly found in LDL were examined since these compounds are believed to play a role in atherogenesis and may be transferred from LDL to vascular cells during lipoprotein uptake. Indications that this really occurs stems from the observations that oxysterols are present in human arteriosclerotic plaques (19, 37, 38) and in human foam cells (39).

The physical effects of LDL oxysterols in DPH-containing vesicles of POPC and DOPC were studied by time-resolved fluorescence depolarization experiments. The analysis of the obtained data with the Brownian diffusion model yields two statistically equivalent solutions that differ only in the value of $\langle P_4 \rangle$. One solution has a high $\langle P_4 \rangle$ value, the other a low value. We note that this ambiguity in the analysis does not occur with the ESR and AFD measurements (23). The distribution function with the higher $\langle P_4 \rangle$ value shows a preferential orientation of the long molecular axes along the normal to the local vesicle surface. The solution with the low $\langle P_4 \rangle$ values exhibits a collective molecular tilt (36). We

TABLE 4. Average fluorescence lifetime of TMA-DPH in POPC vesicles

Lipid	$\langle \tau \rangle$ (ns)
POPC	4.2
POPC + cholesterol	4.7
POPC + 25-hydroxycholesterol	4.4

Average lifetime of TMA-DPH in the indicated lipid mixtures at 20°C using a lipid to probe ratio of 250:1. Lipid vesicles were prepared by sonication. A sterol to phospholipid ratio of 1:20 was used. The uncertainty (68% confidence limit) is 10%.

Downloaded from www.jlr.org by guest, on June 18, 2012

selected the solution with the high $\langle P_4 \rangle$ values, as the low $\langle P_4 \rangle$ solution cannot be reconciled with the result of other physical techniques (40, 41) and the data obtained with ESR and AFD yield only the high $\langle P_4 \rangle$ solution.

In **Table 5** we have listed the order parameters $\langle P_2 \rangle$, $\langle P_4 \rangle$, the diffusion coefficient $D_\perp$, and the average fluorescence lifetime $\langle \tau \rangle$ of DPH in the different lipid bilayers. In POPC vesicles (Table 5) the majority of the oxysterols have, within experimental error, the same $\langle P_2 \rangle$ and $\langle P_4 \rangle$ values as found for cholesterol. Only cholesterol-α-epoxide causes significantly lower $\langle P_4 \rangle$ values than cholesterol. The overall effects of the different sterols are illustrated in Fig. 4, where we have plotted the orientational distribution functions of DPH in vesicles of POPC, POPC + cholesterol, POPC + cholesterol-α-epoxide, and POPC + CO-mix. These curves show that POPC + cholesterol-α-epoxide has a distribution function similar to pure POPC and is disordered compared to membranes containing the same amount of cholesterol. In POPC vesicles, cholesterol and all the investigated oxysterols significantly decrease the rotational diffusion ($D\perp$) of DPH.

In DOPC vesicles, also Table 5, the picture is slightly different. Here the $\langle P_2 \rangle$ values also increase due to the presence of oxysterols, but not to the same extent as with cholesterol. Within experimental error most $\langle P_4 \rangle$ values are the same. The effect of the values of these order parameters on the orientational distribution of DPH in different DOPC-mixtures is shown in **Fig. 5** and **Fig. 6.** The rotational diffusion of DPH in DOPC + oxysterol mixtures is the same or slightly decreased as compared to DOPC + cholesterol. Only 7β-hydroxycholesterol yields $\langle P_2 \rangle$ and $\langle P_4 \rangle$ values that are considerably lower than those for DOPC + cholesterol vesicles while the rotational diffusion is increased as compared to DOPC + cholesterol.

Table 5 shows that the average fluorescence lifetime $\langle \tau \rangle$ of DPH is hardly affected by the presence of 5 mol % cholesterol or oxysterols.

DISCUSSION

Atherogenesis is a complex process in which different cell species of the arterial wall, lipoproteins, and blood platelets play a role and there are many indications that cholesterol oxidation products may be involved in this process, affecting the behavior of cells as well as lipoproteins. Blache and Bontoux (12) found that the exposure of rat blood platelets to 22S-hydroxycholesterol enhances their rate of aggregation, whereas 25-hydroxycholesterol is inhibitory. From this observation the authors suggested that oxysterols work at the membrane

TABLE 5. Effects of oxysterols on molecular order and dynamics of DPH in POPC and DOPC vesicles: time-dependent fluorescence anisotropy measurements

Lipid	$\langle P_2 \rangle$	$\langle P_4 \rangle$	$D_\perp$ (1/ns)	$\langle \tau \rangle$ (ns)
POPC (ref. 39)	0.14	0.28	0.116	8.7
POPC + cholesterol	0.56	0.42	0.042	8.9
POPC + CO-mix	0.52	0.34	0.050	7.7
POPC + cholestanetriol	0.50	0.30	0.047	8.4
POPC + 25-hydroxycholesterol	0.51	0.31	0.044	8.6
POPC + 7-ketocholesterol	0.50	0.30	0.047	8.5
POPC + cholesterol-α-epoxide	0.57	0.20	0.039	8.5
POPC + cholesterol-β-epoxide	0.56	0.33	0.042	8.4
POPC + 7β-hydroxycholesterol	0.53	0.27	0.044	8.4
POPC + 3-5-diene-7-one	0.52	0.28	0.045	7.1
POPC + 7α-hydroxycholesterol	0.52	0.32	0.048	8.5
DOPC	0.00	0.15	0.090	7.9
DOPC + cholesterol	0.6	0.3	0.06	8.0
DOPC + 7β-hydroxycholesterol	0.11	0.20	0.088	6.7
DOPC + 3-5-diene-7-one	0.46	0.25	0.056	7.8
DOPC + CO-mix	0.41	0.17	0.052	7.8
DOPC + cholestanetriol	0.40	0.16	0.052	7.9
DOPC + 25-hydroxycholesterol	0.44	0.22	0.054	8.2
DOPC + cholesterol-β-epoxide	0.46	0.21	0.053	8.0
DOPC + cholesterol-α-epoxide	0.46	0.21	0.052	8.1
DOPC + 7-ketocholesterol	0.46	0.19	0.052	8.1

Structural effects of cholesterol and the indicated cholesterol oxides on lipid vesicles prepared with POPC and DOPC. Lipid vesicles were prepared by sonication. A sterol to lipid ratio of 1:20 was used. The effects of oxysterols in the lipid vesicles were investigated by time-resolved fluorescence anisotropy measurements on DPH at 20°C using a probe ratio of 250:1. The effects are listed in the form of order parameters $\langle P_2 \rangle$ and $\langle P_4 \rangle$ and the dynamic parameter $D_\perp$. Also listed is the average fluorescence lifetime of DPH, $\langle \tau \rangle$. The uncertainties (68% confidence limits) are 15% in $\langle P_2 \rangle$, 25% in $\langle P_4 \rangle$), 30% in $D_\perp$, and 10% in $\langle \tau \rangle$.

Downloaded from www.jlr.org by guest, on June 18, 2012

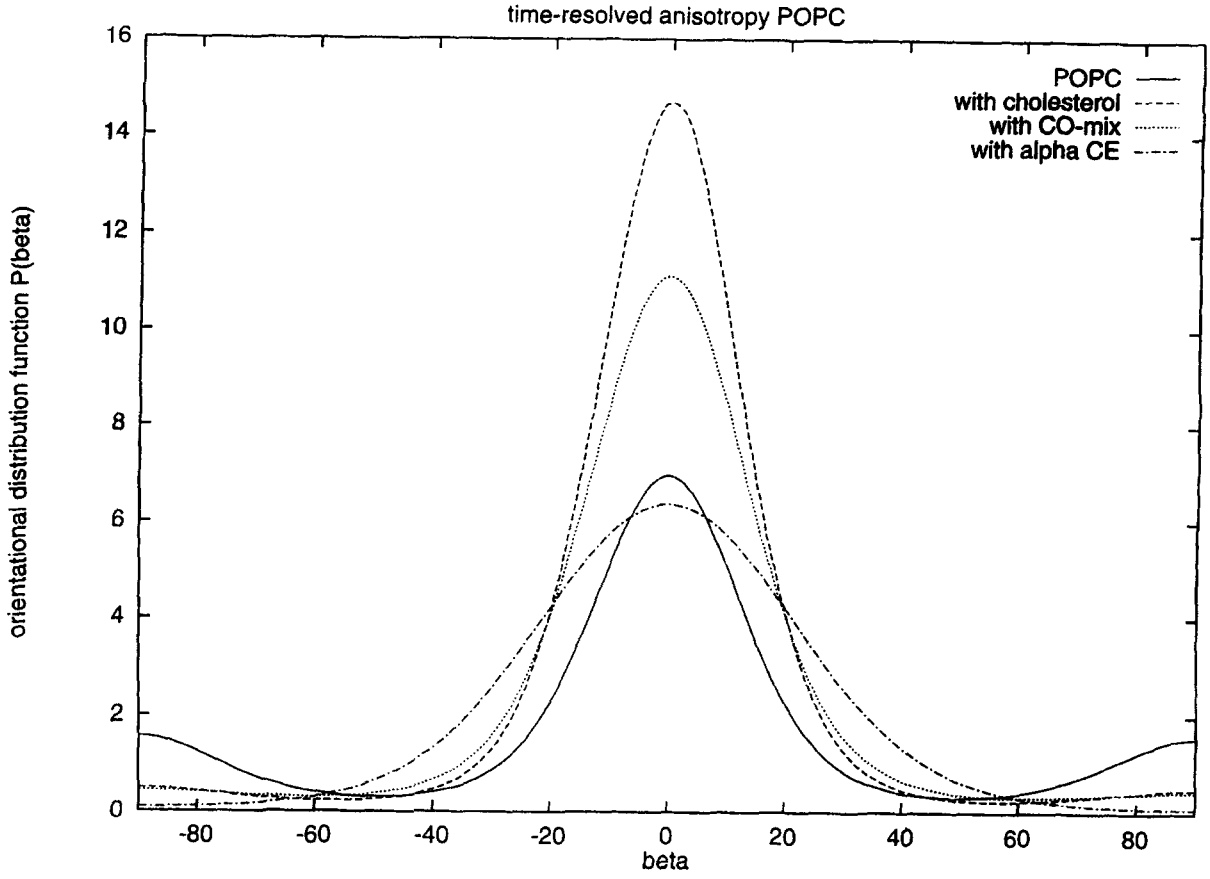

Fig. 4. Orientational distribution functions P(β) of DPH in sonicated vesicles of POPC, POPC + cholesterol, POPC + cholesterol-α-epoxide, and POPC + CO-mix. A sterol to phospholipid ratio of 1:20 was used. The effects of oxysterols in the lipid vesicles were investigated using time-resolved anisotropy measurements on DPH at 20°C using a lipid to probe ratio of 250:1 (see also Table 5).

level, a reasonable assumption as oxysterols are membrane-soluble and by their presence in membranes may be expected to influence their physical properties. This prompted us to study the physical effects of different oxysterols in a pure lipid system to investigate the manner by which oxysterols affect the physical structure of lipid membranes and whether this might explain the effects on blood platelet aggregation. Our measurements on planar POPC membranes with ESR and AFD show that 19-hydroxycholesterol, 22S-hydroxycholesterol, and 25-hydroxycholesterol induce the same structural effects as cholesterol: an increase in molecular order and no change in the rotational dynamics of the investigated probe molecules.

These results, therefore, indicate that the different effects on platelet aggregation between 22S-hydroxycholesterol and 25-hydroxycholesterol cannot, in a straightforward way, be understood by membrane structural effects. It has been hypothesized that oxysterols influence the passive permeability of membranes, for example for calcium ions, and there are several reports which show that 25-hydroxycholesterol increases the permeability of cells and liposomes to calcium ions (42, 43) and glucose (44). The latter authors suggested that the presence of the C25-hydroxylgroup in 25-hydroxycholesterol in the hydrophobic core of the bilayer brings about a perpendicular shuttling of 25-hydroxycholesterol between the inner and the outer monolayer of the membrane. This would cause a local disordering of the membrane lipids leading to the observed high permeability of 25-hydroxycholesterol-containing DOPC liposomes (44). Our results with different probe molecules in planar POPC bilayers and in small unilamellar POPC and DOPC vesicles show, however, that 25-hydroxycholesterol does not induce any disordering. On the contrary, in all systems we investigated 25-hydroxycholesterol had a fairly strong ordering effect in concentrations up to 5 mol %, see Tables 2, 3, and 5. If there was a perpendicular shuttling of 25-hydroxycholesterol between the inner and the outer monolayer of the

Downloaded from www.jlr.org by guest, on June 18, 2012

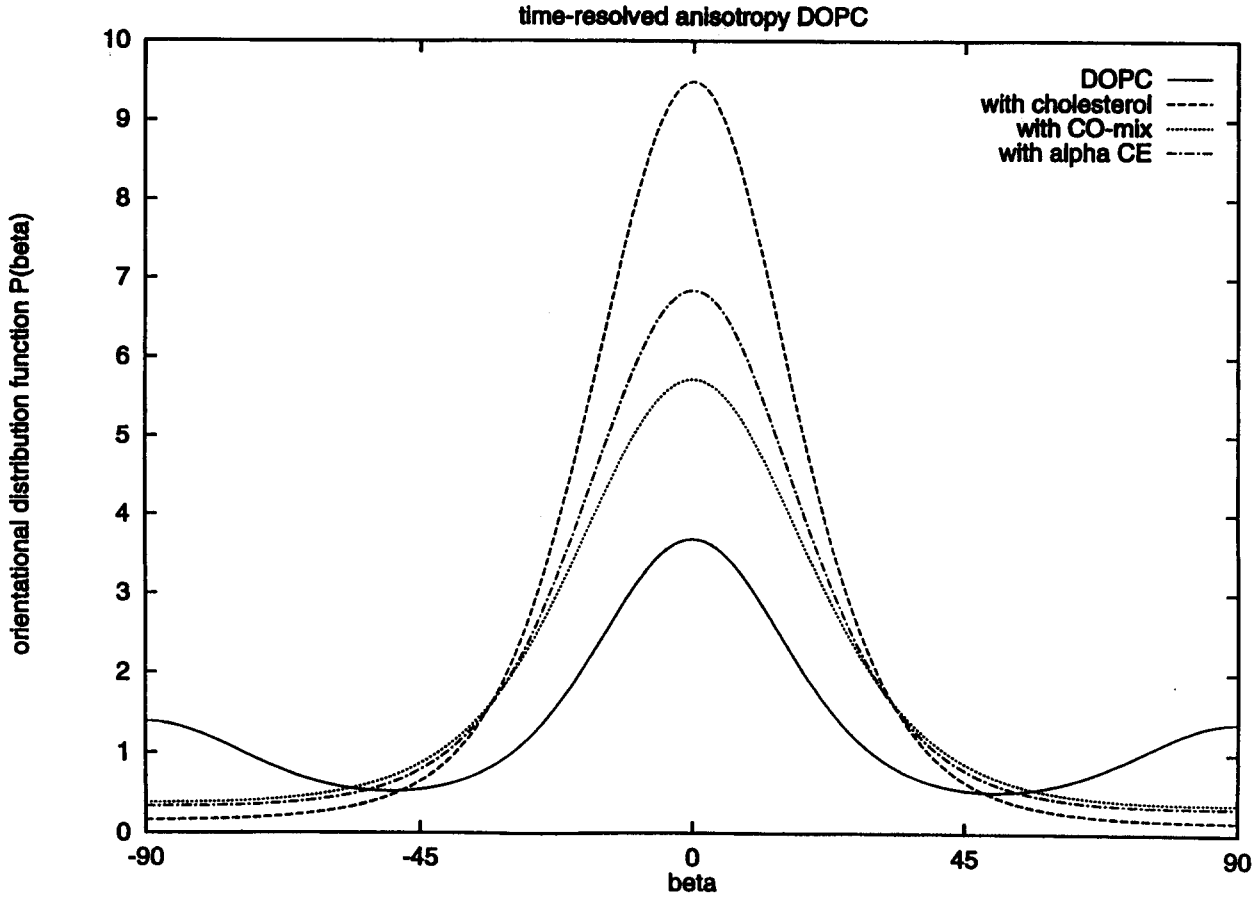

Fig. 5. Orientational distribution functions P(β) of DPH in sonicated vesicles of DOPC, DOPC + cholesterol, DOPC + CO-mix, and DOPC + cholesterol-α-epoxide. A sterol to phospholipid ratio of 1:20 was used. The effects of oxysterols in the lipid vesicles were investigated using time-resolved anisotropy measurements on DPH at 20°C using a lipid to probe ratio of 250:1 (see also Table 5).

membrane, as suggested by Theunissen et al. (44), an increased population of DPH probe molecules at orientations more parallel to the bilayer plane would be expected but was not found in the lipid membranes we studied (Fig. 6). Benga and coworkers (45) and Sinensky (46) have investigated the ordering effects of 25-hydroxycholesterol in egg-lecithin liposomes, using ESR measurements on stearic acid spin probes. They found that 25-hydroxycholesterol at concentrations up to 5 mol % had similar ordering effects as cholesterol in agreement with our findings in Tables 2, 3, and 5. As yet we have no explanation for the increase in order induced by 25-hydroxycholesterol in relation to its permeability enhancing properties. The question can be addressed by Monte Carlo simulations of oxysterols in lipid bilayers, analogous to (47). First results of such simulations on membranes containing 25-hydroxycholesterol suggest that 25-hydroxycholesterol is located in the headgroup region, parallel to the membrane plane. According to the Monte Carlo simulations, the effect is an increase in probe ordering and an increase in membrane permeability (Y. K. Levine, personal communication).

Our data on planar POPC membranes in Tables 2 and 3 indicate that the location of the hydroxyl group on C19, C22, or C25 of the sterol moiety does not affect the ordering properties of these three oxysterols.

The presence of oxysterols in oxidized LDL and in arteriosclerotic lesions and the many observed cytotoxic effects of various oxysterols suggests that cell injury by oxysterols may be attributed to their effects on membranes (3, 5, 6, 7, 9, 14, 42, 43, 48–50). Oxidation of LDL yields a number of oxysterols, the composition of which is shown in Table 1 (from ref. 11). Moreover, oxysterols are also found in human arteriosclerotic plaque and in smooth muscle cells (6, 10, 11, 19). We, therefore, decided to investigate the structural effects of the oxysterols commonly found in oxidized LDL by embedding them in well-defined lipid bilayers. Considering the concentrations of oxysterols encountered in vivo we took a concentration of 5 mol %. The results of time-resolved fluorescence depolarization measurements on

Downloaded from www.jlr.org by guest, on June 18, 2012

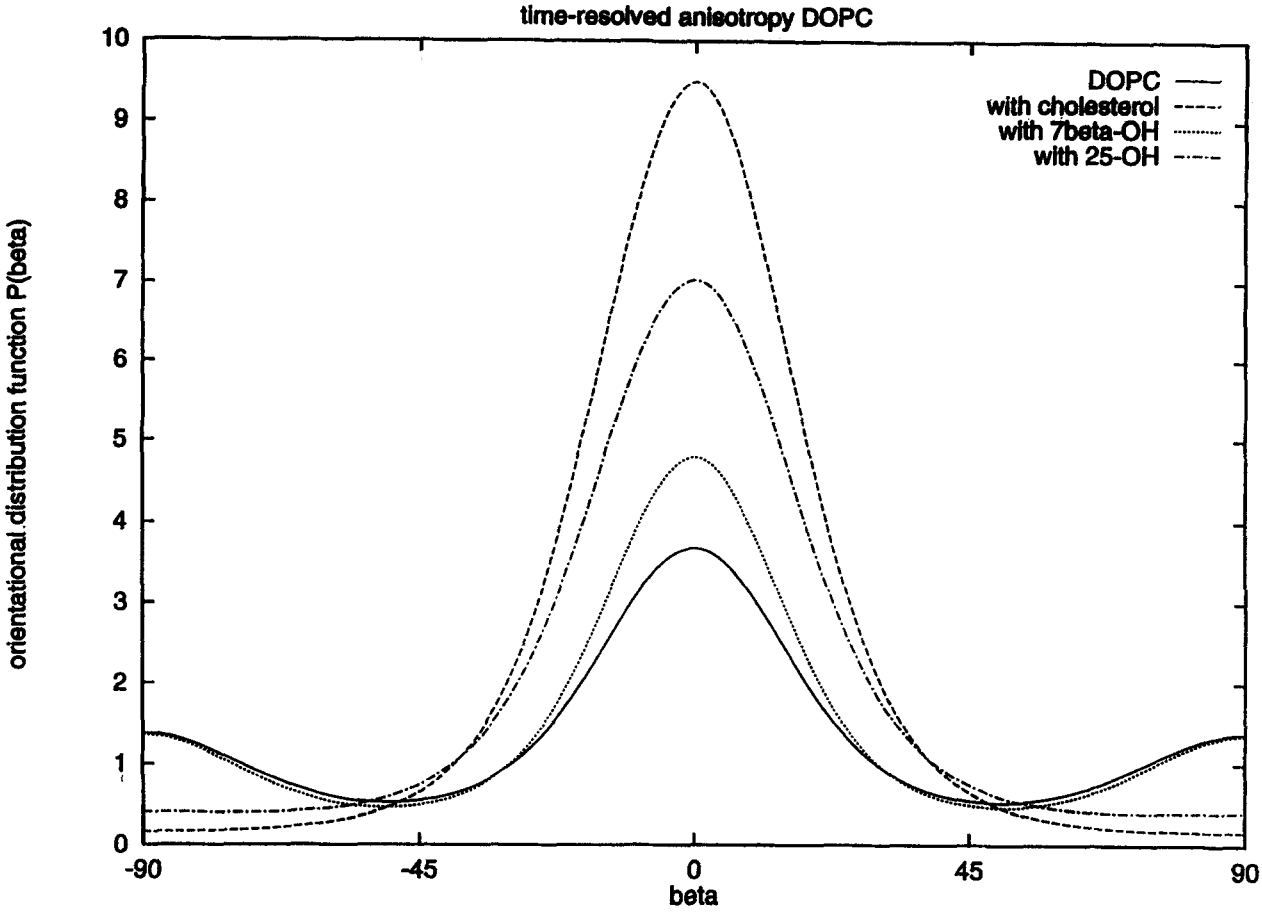

Fig. 6. Orientational distribution functions P(β) of DPH in sonicated vesicles of DOPC, DOPC + cholesterol, DOPC + 7β-hydroxycholesterol, and DOPC + 25-hydroxycholesterol. A sterol to phospholipid ratio of 1:20 was used. The effects of oxysterols in the lipid vesicles were investigated using time-resolved anisotropy measurements on DPH at 20°C using a lipid to probe ratio of 250:1 (see also Table 5).

small unilamellar lipid vesicles of POPC and DOPC (Table 5) show that the majority of the oxysterols produce effects similar to that of cholesterol: an increase in molecular order and a decrease in rotational dynamics of the fluorescent probe molecule DPH. Only cholesterol-α-epoxide causes a significant decrease in order as compared to cholesterol in POPC vesicles. In DOPC vesicles the majority of the investigated LDL-oxysterols produce a slightly lower molecular order than cholesterol while 7β-hydroxycholesterol produces the greatest decrease in molecular order as compared to cholesterol. From these data we conclude that the majority of the investigated oxysterols have cholesterol-like effects, although the amount of ordering is smaller than caused by cholesterol. Of the individual oxysterols, 7β-hydroxycholesterol produces the most pronounced disordering effect in comparison with cholesterol for both POPC and DOPC membrane preparations. This effect coincides with reports by Chisolm et al. (51) who showed that 7β-hydroxycholesterol (derived from 7β-hydroperoxy-cholesterol) was the most toxic oxysterol found in oxidatively modified LDL.

The question now arises how the physical effects of the different oxysterols on model membranes are related to the observed effects on different biological systems (5, 6, 9, 12, 14, 48, 49). In those membranes that contain high amounts of cholesterol, replacement of a part of this cholesterol by one or a mixture of oxysterols may change the permeability of the membrane if the cholesterol/oxysterol mixture significantly affects the overall molecular packing. It is well known that the presence of cholesterol in membranes decreases the permeability of these membranes to different compounds. Considering only the lipid portion of the membrane, a change in permeability brought about by oxysterols due to a local disordering might have profound effects especially for the permeability for calcium ions as recently demonstrated (52), as calcium ions play a crucial role in cell signaling, smooth muscle cell contraction (53, 54), in platelet aggregation (12), in growth

Downloaded from www.jlr.org by guest, on June 18, 2012

factor-induced cell reproduction (55), and likely in apoptosis (56). Small changes in calcium influx may act as a messenger for the induction of further increases in intracellular calcium concentration from internal stores (54). As noted above, there are several reports showing that lipid peroxidation products and oxysterols bring about changes in membrane permeability to calcium ions (7, 9, 42, 43, 50, 57). In a recent paper it was shown that the oxysterol mixture found in oxidized LDL induces a rapid and strong change in calcium permeability in rabbit aortic endothelial cells (52).

Our studies were limited to investigating the structural effects of oxysterols on the lipid part of the membrane. This, of course, does not give insight into the effects of oxysterols brought about by their effects of membrane proteins or cell function which is the goal of future studies.

This work was supported by NIH grant ES 03466 and by NATO grant no. 890966(5-2-05/RG). We thank Drs. David Shaw and Moira Beehan for help with the fluorescence anisotropy measurements with the synchrotron facility in Daresbury (U.K.). The measurements with the synchrotron facility were made possible by the financial support of the EC.

Manuscript received 19 January 1996 and in revised form 29 April 1996.

REFERENCES

1. Smith, L. L. 1981. Cholesterol Oxidation. Plenum Press, New York.
2. Smith, L. L. 1987. Cholesterol autooxidation 1981–1986. *Chem. Phys. Lipids.* **44:** 87–125.
3. Gold, P., S. Grover, and D. A. K. Roncari, editors. 1992. Cholesterol and coronary heart disease. The Parthenon Publishing Group, Lancs, LA6 2LA, UK.
4. Smith, L. L. 1992. The oxidation of cholesterol. *In* Biological Effects of Cholesterol Oxides. S-K. Peng and R. J. Morin, editors. CRC Press, Boca Raton, Ann Arbor, London. 7–31.
5. Sevanian, A., J. Berliner, and H. Peterson. 1991. Uptake, metabolism and cytotoxicity of isomeric cholesterol-5-6-epoxides in rabbit aortic endothelial cells. *J. Lipid Res.* **32:** 147–155.
6. Peng, S-K., A. Sevanian, and R. J. Morin. 1992. Cytotoxicity of cholesterol oxides. *In* Biological Effects of Cholesterol Oxides. S-K. Peng and R. J. Morin, editors. CRC Press, Boca Raton, Ann Arbor, London. 147–166.
7. Sevanian, A., H. Peterson, and T. Coates. 1988. Cytotoxicity of cholesterol oxidation products in bovine and rabbit aortic endothelial cells. *In* Modified Lipoproteins. Proceedings of a satellite meeting of the 8th International Symposium on Atherosclerosis, Venice, October 1988. 103–118.
8. Hughes, H., B. Mathews, M. L. Lenz, and J. R. Guyton. 1994. Cytotoxicity of oxidized LDL to porcine aortic smooth muscle cells is associated with the oxysterols 7-ketocholesterol and 7-hydroxycholesterol. *Arterioscler. Thromb.* **14:** 1177–1185.
9. Peng, S-K., and R. J. Morin. 1992. Effects of cholesterol oxides on cell membranes. *In* Biological Effects of Cholesterol Oxides. S-K. Peng and R. J. Morin, editors. CRC Press, Boca Raton, Ann Arbor, London. 125–145.
10. Steinbrecher, U. P., H. Zhang, and M. Lougheed. 1990. Role of oxidatively modified LDL in artheriosclerosis. *Free Rad. Biol. Med.* **9:** 155–168.
11. Hodis, H. N., D. M. Kramsch, P. Avogaro, G. Bittolo-Bon, G. Cazzolato, J. Hwang, H. Peterson, and A. Sevanian. 1994. Biochemical and cytotoxic characteristics of an in vivo circulating oxidized low density lipoprotein (LDL). *J. Lipid Res.* **35:** 669–677.
12. Blache, D., and G. Bontoux. 1988. Biological effects of oxysterols on platelet function. *Thromb. Res.* **50:** 221–230.
13. Cox, D. C., K. Comai, and A. L. Goldstein. 1988. Effects of cholesterol and 25-hydroxycholesterol on smooth muscle cell and endothelial cell growth. *Lipids.* **23:** 85–88.
14. Pie, J. E., and C. Seillan. 1992. Oxysterols in cultured bovine aortic smooth muscle cells and in the monocyte-like cell line U937. *Lipids.* **27:** 270–274.
15. Sattler, W., J. Christison, and R. Stocker. 1995. Cholesteryl ester hydroperoxide reducing activity associated with isolated high- and low-density lipoproteins. *Free Rad. Biol. Med.* **18:** 421–429.
16. Jialal, I., D. A. Freeman, and S. M. Grundy. 1991. Varying susceptibility of different low density lipoproteins to oxidative modification. *Arterioscler. Thromb.* **11:** 482–488.
17. Lang, J. K., and H. Esterbauer. 1991. Oxidized LDL and atherosclerosis. *In* Membrane Lipid Oxidation. Vol. III. Vigo-Pelfrey, editor. CRC Press, Boca Raton, Ann Arbor, London. 265–282.
18. Palinsky, W., V. A. Ord, A. S. Plump, J. L. Breslow, D. Steinberg, and J. L. Witzum. 1994. ApoE-deficient mice are a model of lipoprotein oxidation in atherogenesis. *Arterioscler. Thromb.* **14:** 605–616.
19. Suarna, C., R. T. Dean, J. May, and R. Stocker. 1995. Human atherosclerotic plaque contains both oxidized lipids and relatively large amounts of α-tocopherol and ascorbate. *Arterioscler. Thromb.* **15:** 1616–1624.
20. van Langen, H., G. van Ginkel, and Y. K. Levine. 1988. A comparison of the molecular dynamics of fluorescent probes in curved lipid vesicles and planar multibilayers. *Liq. Cryst.* **3:** 1301–1317.
21. Korstanje, L. J., E. E. van Faassen, and Y. K. Levine. 1989. Slow-motion ESR study of order and dynamics in oriented lipid multibilayers: effects of unsaturation and hydration. *Biochim. Biophys. Acta.* **980:** 225–233.
22. van Ginkel, G., and A. Sevanian. 1994. Lipid peroxidation-induced membrane structural alteration. *Methods Enzymol.* **233:** 273–288.
23. van Langen, H., G. van Ginkel, D. Shaw, and Y. K. Levine. 1989. The fidelity of response by 1-[4-(trimethylammonio)phenyll-6-phenyl-1,3,5-hexatriene in time-resolved fluorescence anisotropy measurements on lipid vesicles. *Eur. Biophys. J.* **17:** 37–48.
24. Deinum, G., H. van Langen, G. van Ginkel, and Y. K. Levine. 1988. Molecular order and dynamics in planar lipid bilayers: effects of unsaturation and sterols. *Biochemistry.* **27:** 852–860.
25. Mulders, F., H. van Langen, G. van Ginkel, and Y. K. Levine. 1986. The static and dynamic behavior of fluorescent probe molecules in lipid bilayers. *Biochim. Biophys. Acta.* **859:** 209–218.
26. Zannoni, C., A. Arcioni, and P. Cavatorta. 1981. A theory of fluorescence depolarization in membranes. *Mol. Phys.* **42:** 1303–1320.

Downloaded from www.jlr.org by guest, on June 18, 2012

27. Nordio, P. L., and U. Segre. 1979. Rotational dynamics. *In* The Molecular Physics of Liquid Crystals. G. R. Luckhurst and G. W. Gray, editors. Academic Press, New York. 411–426.
28. Wratten, M. L., G. van Ginkel, A. van't Veld, A. Bekker, E. E. van Faassen, and A. Sevanian. 1992. Structural and dynamic effects of oxidatively modified phospholipids in unsaturated lipid membranes. *Biochemistry.* **31:** 10901–10907.
29. Sevanian, A., R. Seraglia, P. Traldi, P. Rossato, F. Ursini, and H. N. Hodis. 1994. Analytical approaches to the measurement of plasma cholesterol oxidation products using gas and high performance liquid chromatography/mass spectrometry. *Free Rad. Biol. Med.* **17:** 397–410.
30. Freed, J. H. 1976. Theory of slow tumbling ESR spectra for nitroxides. *In* Spin Labeling, Theory and Applications. L. J. Berliner, editor. Academic Press, New York. 53–132.
31. Dammers, A. J., Y. K. Levine, and J. A. Tjon. 1988. Numerical simulations of electron spin resonance spectra: unified description and comparison of the Lanczos algorithm, the generalized Mori method, and Padé approximants. *J. Chem. Phys.* **89:** 4505–4513.
32. Freed, J. H., G. V. Bruno, and C. F. Polnaszek. 1971. Electron spin resonance line shapes and saturation in the slow motional region. *J. Phys. Chem.* **58:** 3385–3399.
33. Kubo, R. 1969. A stochastic theory of lineshcape. *In* Stochastic Processes in Chemical Physics. K. Shuler, editor. Interscience, New York, London, Sydney, Toronto. 101–128.
34. Press, W. H., B. P. Flannery, S. A. Teukolsky, and W. T. Vetterling. 1989. Numerical Recipes in Pascal. Cambridge University Press, Cambridge, New York, Port Chester, Melbourne, Sydney. Chapter 14.4, 14.5. 572–590.
35. Beechem, J. M. 1992. Global analysis of biochemical and biophysical data. *Methods Enzymol.* **210:** 37–54.
36. Van Langen, H., Y. K. Levine, M. Ameloot, and H. Pottel. 1987. Ambiguities in the interpretation of time-resolved fluorescence anisotropy measurements on lipid vesicle systems. *Chem. Phys. Lett.* **140:** 394–400.
37. Carpenter, K. L., J. A. Taylor, B. Ballantine, B. Fussell, B. Halliwell, and M. J. Mitchinson. 1993. Lipids and oxidised lipids in human atheroma and normal aorta. *Biochim. Biophys. Acta.* **1167:** 121–130.
38. Smith, L. L., and B. H. Johnson. 1989. Biological activities of oxysterols. *Free Rad. Biol. Med.* **7:** 285–332.
39. Mattson, L. 1994. Studies of arterial-derived foam cells in atherogenesis. University of Goteborg, Ph.D. Thesis.
40. Hemminga, M. A. 1983. Interpretation of ESR and saturation transfer ESR spectra of spin-labeled lipids and membranes. *Chem. Phys. Lipids.* **32:** 179.
41. Grell, E., editor. 1981. Membrane Spectroscopy. Springer-Verlag, Berlin.
42. Holme, R. P., and N. L. Yoss. 1984. 25-Hydroxysterols increase the permeability of liposomes to Ca and other cations. *Biochim. Biophys. Acta.* **770:** 15–21.
43. Boissonneault, G. A., and H. J. Heininger. 1985. 25-Hydroxycholesterol-induced elevations in ^{45}Ca uptake: permeability changes in P815 cells. *J. Cell. Physiol.* **125:** 471–475.
44. Theunissen, J. J. H., R. L. Jackson, H. J. M. Kempen, and R. A. Demel. 1986. Membrane properties of oxysterols, interfacial orientation, influence on membrane permeability and redistribution between membranes. *Biochim. Biophys. Acta.* **860:** 66–74.
45. Benga, G., A. Hodârnălau, M. Ionescu, V. I. Pop, P. T. Frangopol, V. Strujan, R. P. Holmes, and F. A. Kummerow. 1983. A comparison of the effects of cholesterol and 25-hydroxycholesterol on egg yolk lecithin liposomes: spin label studies. *Ann. NY Acad. Sci.* **414:** 140–152.
46. Sinensky, M. 1981. A comparison of solution properties of cholesterol and 25-hydroxycholesterol. *Arch. Biochem. Biophys.* **209:** 321–324.
47. Levine, Y. K. 1993. Monte Carlo dynamics study of *cis* and *trans* unsaturated hydrogen chains. *Mol. Phys.* **78:** 619–628.
48. Kucuk, O., L. J. Lis, T. Dey, R. Mata, M. P. Westerman, S. Yachnin, R. Szostek, D. Tracy, J. W. Kauffman, D. A. Gage, and C. C. Sweeley. 1992. The effects of cholesterol oxidation products in sickle and normal red blood cell membranes. *Biochim. Biophys. Acta.* **1103:** 296–302.
49. Parish, E. J., V. B. B. Nanduri, H. H. Kohl, and F. R. Taylor. 1986. Oxysterols: chemical synthesis, biosynthesis and biological activities. *Lipids.* **21:** 27–30.
50. Sevanian, A., H. N. Hodis, J. Hwang, and H. Peterson. 1995. Involvement of cholesterol oxides in the atherogenic action of oxidized LDL. *In* Free Radicals, Lipoprotein Oxidation and Artherosclerosis. G. Bellomo, G. Finardi, E. Maggi, and C. Rice-Evans, editors. Richelieu Press, London. 139–161.
51. Chisolm, G. M., G. Ma, K. C. Irwin, L. L. Martin, K. G. Gunderson, L. F. Linberg, D. W. Morel, and P. E. DiCorleto. 1994. 7β-Hydroperoxycholest-5-en-3β-ol, a component of human atherosclerotic lesions, is the primary cytotoxin of oxidized human low density lipoprotein. *Proc. Natl. Acad. Sci. USA.* **91:** 11452–11456.
52. Sevanian, A., H. N. Hodis, J. Hwang, L. L. McLeod, and H. Peterson. 1995. Characterization of endothelial cell injury by cholesterol oxidation products found in oxidized LDL. *J. Lipid Res.* **36:** 1971–1986.
53. Brenner, B. 1990. Muscle mechanics and biochemical kinetics. *In* Molecular Mechanisms in Muscle Contraction, J. M. Squire, editor. McMillan Press, Basingstoke, Hampshire. 77–149.
54. Rüegg, J. C. 1986. Calcium in Muscle Activation, A Comparative Approach. Springer-Verlag, Berlin.
55. Boonstra, J., P. Rijken, B. Humbel, F. Cremers, A. Verkleij, and P. van Bergen en Henegouwen. 1995. The epidermal growth factor. *Cell Biol. Int.* **19:** 413–430.
56. Bast, A. 1993. Oxidative stress and calcium homeostasis. *In* DNA and Free Radicals. B. Halliway and O. I. Aruoma, editors. Ellis Horwood Limited, Chinchester. 95–108.
57. Levitsky, D. O., A. V. Lebedev, A. V. Kuzmin, and V. M. Brovkovich. 1988. Role of the lipid peroxidations in increasing calcium permeability of model and natural membranes. *In* The Role of Oxygen Radicals in Cardiovascular Diseases. A. L'Abbate and F. Ursini, editors. Kluwer Academic Publishers, Dordrecht, Boston, London. 127–141.

Downloaded from www.jlr.org by guest, on June 18, 2012